Simplified Dynamic Models for Control of Riser Slugging in Offshore Oil Production

Esmaeil Jahanshahi and **Sigurd Skogestad,** Norwegian University of Science and Technology

Summary

Elaborated models, such as those used for simulation purposes [e.g., in the OLGA® simulator (Bendiksen et al. 1991)], cannot be used for model-based control design because these models use too many state variables and the model equations are not usually available for the user. The focus of this paper is on deriving simple, dynamical models with few state variables that capture the essential dynamic behavior for control. We propose a new simplified dynamic model for severe-slugging flow in pipeline/riser systems. The proposed model, together with five other simplified models found in the literature, are compared with results from the OLGA simulator. The new model can be extended to other cases, and we consider also a well/pipeline/riser system. The proposed simple models are able to represent the main dynamics of severe-slugging flow and compare well with experiments and OLGA simulations.

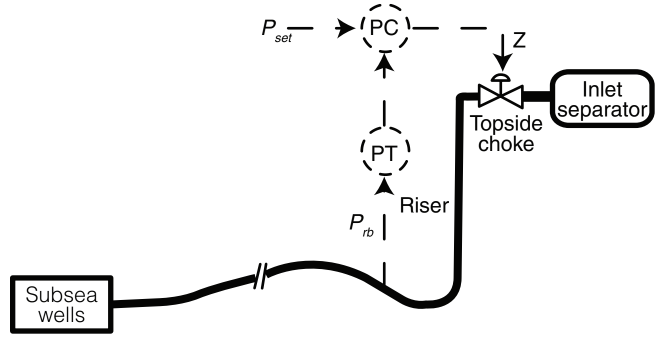

Fig. 1—Preventing slug flow by control of riser-base pressure. (PC=pressure controller and PT=pressure transmitter.)

Introduction

Severe-slugging-flow regimes usually occur in pipeline/riser systems that transport a mixture of oil and gas from the seabed to the surface (Taitel 1986). Such flow regimes, also referred to as "riser slugging," are characterized by severe flow and pressure oscillations. Slugging problems have also been observed in gas lifted oil wells in which two types of instabilities—casing heading and density wave instability—have been reported (e.g., Hu and Golan 2003).

Slugging has been recognized as a serious problem in offshore oil fields because the irregular flow caused by slugging can cause serious operational problems for downstream surface facilities (e.g., overflow of inlet separators). Therefore, effective methods to handle or remove riser slugging are needed, and many efforts have been made to prevent such occurrences (Courbot 1996; Havre et al. 2000). The conventional solution is to partially close the topside choke valve (choking), but this may reduce the production rate, especially for fields in which the reservoir pressure is relatively low. Therefore, a solution that guarantees stable flow and the maximum possible production rate is desirable.

Fortunately, automatic feedback control has been shown to be an effective strategy to eliminate the slugging problem. As shown in **Fig. 1,** the topside choke valve is usually used as the manipulated variable to regulate (control) the riser-base pressure (P_{rb}) at a given pressure set point (P_{set}). Such a system is referred to as "antislug control," and it aims at stabilizing the flow in the pipeline at the operating conditions that, without control, would lead to riser slugging. Different antislug-control strategies have been tested in practice (Havre et al. 2000) and experimentally (Godhavn et al. 2005).

OLGA is a commercial multiphase simulator used widely in the oil industry (Bendiksen et al. 1991). When the development of this simulator was initiated in the 1980s, one of motivations was to study the dynamics of slow flow regimes for offshore oil fields. There has been some research on riser slugging conducted with the OLGA simulator to test antislug control (Fard et al. 2006); however, the model equations coded in commercial simulators are not openly available and appear as a black box to the end user. In addition, the OLGA simulator uses numerous correlations with parameters that are calibrated on the basis of field data. The OLGA simulator works by discretizing the pipe into multiple segments. The model accuracy increases by increasing the number of the segments, but this results in many ordinary-differential equations (ODEs). However, for controller design, we need a fully known and preferably simple model with as few ODEs as possible. When we refer to simple models in this paper, the number of ODEs, or equivalently, the number of "states," will be called "dimensions" of the model.

The focus of this paper is on deriving a simple dynamical model that captures the essential behavior for control—namely, the onset of slugging, not the slugging itself. The aim is to avoid the slug flow regime and, instead, operate at a steady- (nonslug-) flow regime. Therefore, the shape and length of the slugs are not the main concerns in this modeling.

For simplicity, two-phase flow (gas phase and bulk liquid phase) is assumed in the model. To use the model for a three-phase gas/oil/water system, the bulk liquid phase includes the oil and water. As an approximation, the density and other parameters for the bulk liquid phase are the weighted averages (based on volume fractions) of the parameters for the oil and water phases. We also need to ignore the slip between oil and water phases. This approximation should not affect the prediction of slugging onset significantly, except for special cases in which the slip velocity between the water and oil phases exceeds a certain value that is beyond the scope of this study. In such cases, a slip model must be included to improve the model prediction.

Five simplified dynamical models for the pipeline/riser systems were found in the literature. The "Storkaas model" (Storkaas et al. 2003) is a 3D state-space model that has been used for controllability analysis (Storkaas and Skogestad 2007). The "Eikrem model" (Tuvnes 2008; Eikrem 2008) is a 4D state-space model. Another sim-

Original SPE manuscript received for review 16 December 2013. Revised manuscript received for review 22 July 2014. Paper (SPE 172998) peer approved 7 August 2014.

plified model, referred to as the "Kaasa model" (Kaasa et al. 2008), predicts the pressure at the bottom of the riser only. The "Nydal model" (Martins da Silva et al. 2010) is the only model that includes friction in the pipes. The most recently published simplified model is the "Di Meglio model" (Di Meglio et al. 2009, 2010). In addition, we present in this paper a new four-state model that includes features of the other five models. The six models are simulated in the time domain and compared with results from the more-detailed OLGA model in the following five aspects, listed in order of importance:

- Critical valve opening for onset of slugging
- Frequency of oscillations at the critical point (onset of slugging)
- Dynamical response to a step change in the valve opening (nonslug regime)
- Steady-state pressure and flow-rate values (nonslug regime)
- Maximum and minimum (pressure and flow rate) of the oscillations (slug regime)

The simplified models are also analyzed linearly in the frequency domain, where we consider the location of unstable poles and important unstable (right-half-plane) zeroes in the model. The results presented in this paper have been partially presented by Jahanshahi and Skogestad (2011) and Jahanshahi et al. (2012). In the present paper, we compare the new model with the experiments, and we extend it to a well/pipeline/riser system.

This paper is organized as follows. First, we present our new simplified model for pipeline/riser systems. Then, we compare the proposed model and the other simple models with the results from the OLGA simulator and experiments. Finally, we extend this model to well/pipeline/riser systems and compare the extended model with OLGA simulations.

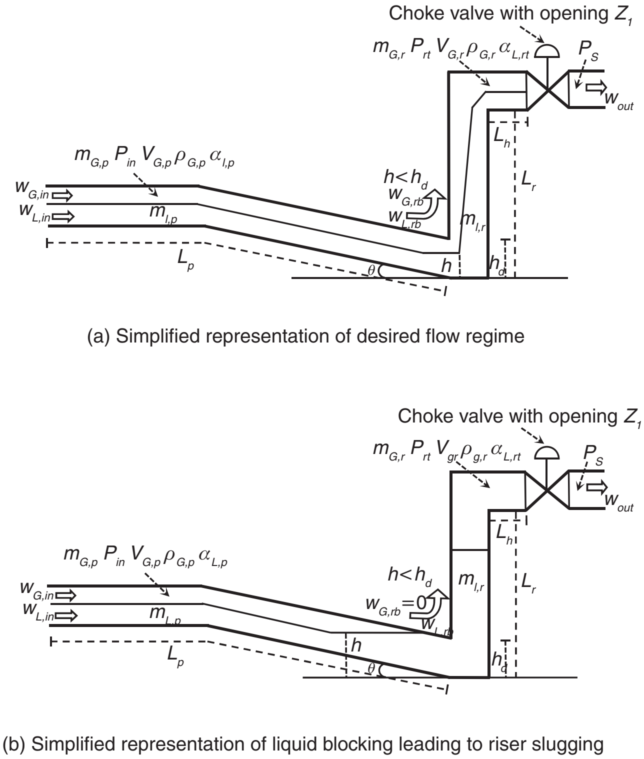

Fig. 2—Pipeline/riser system with important parameters.

New Simplified Four-State Model

Mass-Balance Equations for Pipeline and Riser. For the new simplified model, consider the schematic of the system presented in **Fig. 2.** The four differential equations in the proposed model are simply the mass-conservation law for the gas and liquid phases in the pipeline and riser sections:

$$\frac{\mathrm{d}(m_G)_p}{\mathrm{d}t} = (w_G)_{\mathrm{in}} - (w_G)_{rb}, \quad (1a)$$

$$\frac{\mathrm{d}(m_L)_p}{\mathrm{d}t} = (w_L)_{\mathrm{in}} - (w_L)_{rb}, \quad (1b)$$

$$\frac{\mathrm{d}(m_G)_r}{\mathrm{d}t} = (w_G)_{rb} - (w_G)_{\mathrm{out}}, \quad (1c)$$

and

$$\frac{\mathrm{d}(m_L)_r}{\mathrm{d}t} = (w_L)_{rb} - (w_L)_{\mathrm{out}}, \quad (1d)$$

The four state variables in the model are
$(m_G)_p$ = mass of gas in the pipeline, kg
$(m_L)_p$ = mass of liquid in the pipeline, kg
$(m_G)_r$ = mass of gas in the riser, kg
$(m_L)_r$ = mass of liquid in the riser, kg

The state variables are masses; therefore, they are non-negative values. The time derivatives of the state variables appear on the left side of the state equations (Eqs. 1a through 1d). On the right side of the state equations, w (kg/s) denotes mass-flow rate, and the subscripts "in," "rb," and "out" stand for "inlet," "riser base," and "outlet," respectively. The flow rates on the right side are calculated by the additional model equations that are described later.

Boundary Conditions. ***Inlet conditions.*** In Eqs. 1a and 1b, $(w_G)_{\mathrm{in}}$ and $(w_L)_{\mathrm{in}}$ are the inlet gas and liquid mass-flow rates. They are assumed to be constant in the four-state model, but the inlet boundary conditions are changed in the extended model to make the inlet flow a function of inlet pressure (i.e., reservoir flowing pressure).

Outlet Conditions. We consider a constant pressure (separator pressure, P_s) as the outlet boundary condition, and a simple choke-valve equation determines the outflow of the two-phase mixture:

$$w_{\mathrm{out}} = C_{v1} f(z_1) \sqrt{\rho_{rt} \max(P_{rt} - P_s, 0)}, \quad (2)$$

Here, $0<z_1<1$ is the normalized valve opening (we use Z_1 when the valve opening is given in percentage—$0<Z_1<100$) and $f(z_1)$ is the characteristic equation of the valve. In our simulations, a linear valve is used [i.e., $f(z_1)=z_1$], but this should be changed for other valve types. The individual outlet mass-flow rates of liquid and gas, respectively, are calculated as follows:

$$(w_L)_{\mathrm{out}} = (\alpha_L^m)_{rt}\, w_{\mathrm{out}}, \quad (3)$$

and

$$(w_G)_{\mathrm{out}} = \left[1 - (\alpha_L^m)_{rt}\right] w_{\mathrm{out}}, \quad (4)$$

Here, $(\alpha_L^m)_{rt}$ (kg/kg) is the liquid mass fraction at the top of the riser, which is given by

$$(\alpha_L^m)_{rt} = \frac{(\alpha_L)_{rt}\, \rho_L}{(\alpha_L)_{rt}\, \rho_L + \left[1 - (\alpha_L)_{rt}\right](\rho_G)_r}, \quad (5)$$

where an incompressible liquid phase is assumed (i.e., ρ_L is constant). The density of the two-phase mixture at the top of the riser in Eq. 2 is

$$\rho_{rt} = (\alpha_L)_{rt}\,\rho_L + \left[1-(\alpha_L)_{rt}\right](\rho_G)_r, \quad (6)$$

The liquid volume fraction $(\alpha_L)_{rt}$ (m^3/m^3) in Eqs. 5 and 6 is calculated by Eq. 41. Note that subscript *rt* is used to denote "riser top" and subscript *r* is used to denote "riser."

Pipeline Model. The liquid volume fraction α_L in the pipeline section is given by the liquid mass fraction α_L^m and densities of the two phases (Brill and Beggs 1991): $\alpha_L = \dfrac{\alpha_L^m/\rho_L}{\alpha_L^m/\rho_L + \left(1-\alpha_L^m\right)/\rho_G}$. The average liquid mass fraction in the pipeline section is assumed to be given by the inflow boundary condition $\left\langle \alpha_L^m \right\rangle_p = \dfrac{(w_L)_{\text{in}}}{(w_L)_{\text{in}} + (w_G)_{\text{in}}}$. Throughout this paper, $\langle\,\rangle$ denotes the average operator. The average liquid volume fraction in the pipeline is then

$$\left\langle \alpha_L \right\rangle_p = \frac{\left\langle \rho_G \right\rangle_p (w_L)_{\text{in}}}{\left\langle \rho_G \right\rangle_p (w_L)_{\text{in}} + \rho_L (w_G)_{\text{in}}}, \quad (7)$$

The average gas density $\langle\rho_G\rangle_p$ is calculated on the basis of the nominal (steady-state) pressure in the pipeline by assuming ideal gas,

$$\left\langle \rho_G \right\rangle_p = \frac{P_{\text{in, nom}} M_G}{RT_p}, \quad (8)$$

Eq. 8 is simply $PV=nZRT$, and by "ideal gas," we mean near-nitrogen behavior during which the compressibility factor is equal to unity ($Z=1$). M_G is the gas molecular weight, and $P_{\text{in,nom}}$, which itself depends on $\langle\alpha_L\rangle_p$, is calculated from a steady-state solution of the combined equations for the overall model. By use of Eq. 8 and constant (nominal) inflow rates, we obtain $\langle\alpha_L\rangle_p$ in Eq. 7 as a constant parameter. Note that the constant gas density $\langle\rho_G\rangle_p$ in Eq. 7 is used to obtain a constant $\langle\alpha_L\rangle_p$ only; the gas density in the pipeline is $(\rho_G)_p$, which we will see later.

The cross-sectional area of the pipeline is $A=(\pi/4)D_p^2$, where D_p is the diameter of the pipeline and the volume of the pipeline is $V_p=A_pL_p$. When gas and liquid are distributed homogeneously along the pipeline, the average mass of liquid in the pipeline is

$$\left\langle m_L \right\rangle_p = \rho_L V_p \left\langle \alpha_L \right\rangle_p, \quad (9)$$

With this assumption, the level of liquid in the pipeline at the low point is given by $\langle h\rangle \approx h_d \left\langle \alpha_L \right\rangle_p$, where $h_d=D_p/\cos(\theta)$ is the pipeline opening at the riser base and θ is the pipe inclination with respect to the horizontal ($0°\leq\theta<90°$) at the low point. More precisely, we use in the model

$$\langle h\rangle = K_h h_d \left\langle \alpha_L \right\rangle_p, \quad (10)$$

where K_h is a correction factor approximately equal to unity that can be used to fine tune the model. (Note that in our experience of fitting the model to different pipeline/riser systems, $0.5<K_h\leq1$ usually results in a good fit.) If the liquid content of the pipeline increases by $\Delta(m_L)_p$, it starts to fill up the pipeline from the low point. A length of pipeline equal to ΔL will be occupied by only liquid, where $\Delta(m_L)_p = (m_L)_p - \langle m_L\rangle_p = \Delta L A_p\left(1-\langle\alpha_L\rangle_p\right)\rho_L$ and the level of liquid in the pipeline becomes $h = \langle h\rangle + \Delta L\ \sin(\theta)$ or

$$h = \langle h\rangle + \left[\frac{(m_L)_p - \langle m_L\rangle_p}{A_p\left(1-\langle\alpha_L\rangle_p\right)\rho_L}\right]\sin(\theta), \quad (11)$$

Thus, the level of liquid in the pipeline h can be written as a function of liquid mass in the pipeline $(m_L)_p$, which is a state variable of the model. The remaining parameters in Eq. 11 are constants.

The pipeline gas density is $(\rho_G)_p=(m_G)_p/(V_G)_p$, where the volume occupied by gas in the pipeline is $(V_G)_p=V_p-(m_L)_p/\rho_L$. The pressure at the inlet of the pipeline, assuming ideal gas, is

$$P_{\text{in}} = \frac{(\rho_G)_p RT_p}{M_G}, \quad (12)$$

We consider only the liquid phase when calculating the frictional pressure loss in the pipeline (Brill and Beggs 1991).

$$\left(\Delta P_f\right)_p = \frac{\lambda_p \rho_L \left\langle u_{sL}\right\rangle_p^2 L_p}{2D_p}, \quad (13)$$

Here, λ_p is the friction factor of the pipeline. The correlation developed by Drew et al. (1932) for turbulent flow in smooth-wall pipes is used as the friction factor in the pipeline:

$$\lambda_p = 0.0056 + 0.5\left(N_{\text{Re}}\right)_p^{-0.32}, \quad (14)$$

This is also the equation recommended by Dukler et al. (1964) in their horizontal two-phase-flow correlation (Brill and Beggs 1991). We tried different correlations, and this provides the best numerical enclosure for our simplified model. The correlations considering the pipe roughness lead to a very large friction loss because of the long pipeline. In Eq. 14, the mixture Reynolds number is

$$\left(N_{\text{Re}}\right)_p = \frac{\left\langle\rho_m\right\rangle_p \left\langle U_m\right\rangle_p D_p}{\left\langle\mu_m\right\rangle_p}, \quad (15)$$

where the average mixture density is given by

$$\left\langle\rho_m\right\rangle_p = \left\langle\alpha_L\right\rangle_p \rho_L + \left(1-\left\langle\alpha_L\right\rangle_p\right)(\rho_G)_p, \quad (16)$$

and $\left\langle\mu_m\right\rangle_p$ is the average mixture viscosity,

$$\left\langle\mu_m\right\rangle_p = \left\langle\alpha_L\right\rangle_p \mu_L + \left(1-\left\langle\alpha_L\right\rangle_p\right)\mu_G, \quad (17)$$

We define the mixture velocity by use of superficial velocities, $\left\langle U_m\right\rangle_p = \left\langle U_{sL}\right\rangle_p + \left\langle U_{sG}\right\rangle_p$, where

$$\left\langle U_{sG}\right\rangle_p = \frac{(w_G)_{\text{in}}}{(\rho_G)_p A_p} \quad (18)$$

and

$$\left\langle U_{sL}\right\rangle_p = \frac{(w_L)_{\text{in}}}{\rho_L A_p}, \quad (19)$$

Riser Model. The total volume of the riser, including the horizontal section, is

$$V_r = A_r\left(L_r + L_h\right), \qquad (20)$$

where $A_r = (\pi/4)D_r^2$ is the cross-sectional area of the riser. The volume occupied by gas in the riser is

$$\left(V_G\right)_r = V_r - \left(m_L\right)_r / \rho_L, \qquad (21)$$

and the density of gas in the riser is $(\rho_G)_r=(m_G)_r/(V_G)_r$. Then, the pressure at the top of the riser from the ideal-gas law becomes

$$P_{rt} = \frac{\left(\rho_G\right)_r RT_r}{M_G}, \qquad (22)$$

The average liquid volume fraction in the riser is

$$\left\langle \alpha_L \right\rangle_r = \frac{\left(m_L\right)_r}{\left(V_r \rho_L\right)}, \qquad (23)$$

and the average density of the mixture inside the riser is

$$\left\langle \rho_m \right\rangle_r = \frac{\left(m_G\right)_r + \left(m_L\right)_r}{V_r}, \qquad (24)$$

The friction loss in the riser is

$$\left(\Delta P_f\right)_r = \frac{\lambda_r \left\langle \rho_m \right\rangle_r \left\langle U_m \right\rangle_r^2 \left(L_r + L_h\right)}{2D_r}, \qquad (25)$$

where the friction factor λ_r is computed from an explicit approximation of the implicit Colebrook-White equation (Haaland 1983):

$$\frac{1}{\sqrt{\lambda_r}} = -1.8\log_{10}\left[\left(\frac{\varepsilon/D_r}{3.7}\right)^{1.11} + \frac{6.9}{\left(N_{\text{Re}}\right)_r}\right], \qquad (26)$$

where the Reynolds number for the flow in the riser is

$$\left(N_{\text{Re}}\right)_r = \frac{\left\langle \rho_m \right\rangle_r \left\langle U_m \right\rangle_r D_r}{\left\langle \mu_m \right\rangle_r}, \qquad (27)$$

The average mixture velocity in the riser is $\left\langle U_m \right\rangle_r = \left\langle U_{sL} \right\rangle_r + \left\langle U_{sG} \right\rangle_r$, where

$$\left\langle U_{sL} \right\rangle_r = \frac{\left(w_L\right)_{\text{in}}}{\rho_L A_r} \qquad (28)$$

and

$$\left\langle U_{sG} \right\rangle_r = \frac{\left(w_G\right)_{\text{in}}}{\left(\rho_G\right)_r A_r}, \qquad (29)$$

In Eq. 27, $\left\langle \mu_m \right\rangle_r$ is the average mixture viscosity,

$$\left\langle \mu_m \right\rangle_r = \left\langle \alpha_L \right\rangle_r \mu_L + \left(1 - \left\langle \alpha_L \right\rangle_r\right)\mu_G . \qquad (30)$$

Gas-Flow Model at the Riser Base. As illustrated in Fig. 2b, when the liquid level in the pipeline section exceeds the openings of the pipeline at the riser base ($h>h_d$), the liquid phase obstructs the flow at the low point by competent bridging of the conduit and the gas-flow rate $(w_G)_{rb}$ at the riser base becomes zero,

$$\left(w_G\right)_{rb} = 0, \quad h \ge h_d . \qquad (31)$$

When the liquid is not blocking at the low point ($h<h_d$ in Fig. 2a), the gas will flow from the volume $(V_G)_p$ to $(V_G)_r$ with a mass rate $(w_G)_{rb}$ (kg/s), which is assumed to be given by an "orifice equation" (e.g., Skogestad 2009):

$$\left(w_G\right)_{rb} = K_G A_G \sqrt{\left(\rho_G\right)_p \Delta P_G}, \quad h < h_d, \qquad (32)$$

where

$$\Delta P_G = P_{\text{in}} - \left(\Delta P_f\right)_p - P_{rt} - \left\langle \rho_m \right\rangle_r gL_r - \left(\Delta P_f\right)_r, \qquad (33)$$

The free area for gas (A_G) can be calculated precisely with trigonometric functions (Storkaas et al. 2003):

$$A_G = r_1^2\left[\pi - \phi - \cos\left(\pi - \phi\right)\sin\left(\pi - \phi\right)\right], \qquad (34)$$

where

$$\phi = \pi - \text{acos}\left[1 - \frac{\left(h_d - h\right)\cos\left(\theta\right)}{r_1}\right], \qquad (35)$$

Fig. 3 shows A_G as a function of the liquid level h on the basis of the accurate relationships in Eqs. 34 and 35 as well as the linear and quadratic approximations for this function. The linear approximation is closer to the accurate trigonometric function, but the quadratic approximation leads to a more-accurate onset of slugging. For simplicity, the quadratic approximation is used in this model,

$$A_G = \begin{cases} A_p\left(\dfrac{h_d - h}{h_d}\right)^2, & \text{if } h < h_d \\ 0, & \text{if } h \ge h_d \end{cases}, \qquad (36)$$

Eq. 36 is the approximation of the free area for the gas flow by a triangle, as shown in **Fig. 4.**

Liquid-Flow Model at the Riser Base. The liquid mass-flow rate at the riser base is also described by an orifice equation:

$$\left(w_L\right)_{rb} = K_L A_L \sqrt{\rho_L \Delta P_L}, \qquad (37)$$

where

$$\Delta P_L = P_{\text{in}} - \left(\Delta P_f\right)_p + \rho_L gh - P_{rt} - \left\langle \rho_m \right\rangle_r gL_r - \left(\Delta P_f\right)_r \qquad (38)$$

and

$$A_L = A_p - A_G, \qquad (39)$$

Phase-Distribution Model at the Outlet Choke Valve. To calculate the mass-flow rates of the individual phases as given in Eqs. 2 through 6, the phase distribution at the top of the riser must be known. The liquid volume fraction at the top of the riser $(\alpha_L)_{rt}$ can be calculated by the entrainment model proposed by Storkaas et al. (2003), but their entrainment equations are complicated, which makes the model stiff for numerical solvers. By stiffness, we mean that the entrainment equations lead to rapid variations in the solution of the ordinary-differential equations. This makes the numerical solvers numerically unstable, unless the step size is chosen to be extremely small.

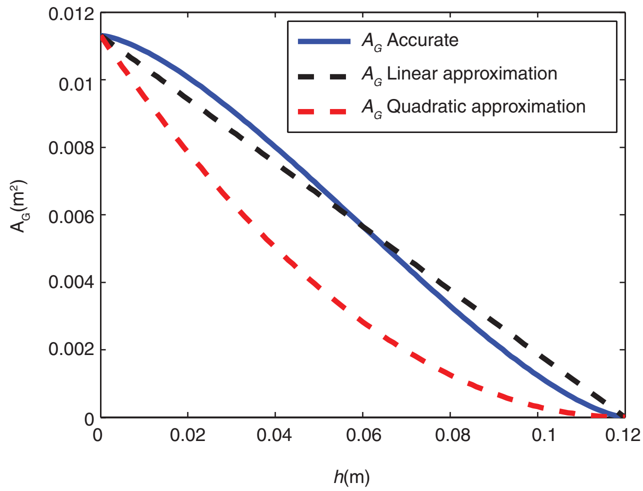

Fig. 3—Approximation of free area for gas flow.

Instead of the entrainment model, we use the knowledge that in a vertical gravity-dominant two-phase pipeline, there is an approximately linear relationship between the pressure and the liquid volume fraction. This has also been observed in OLGA simulations. In addition, the pressure gradient is assumed constant along the riser for the desired nonslugging flow regimes, which then gives that the liquid-volume-fraction gradient is constant (that is, $\frac{\partial(\alpha_L)_r}{\partial y} = \text{constant}$). It then follows that the average liquid volume fraction in the riser is

$$\langle\alpha_L\rangle_r = \frac{(\alpha_L)_{rt} + (\alpha_L)_{rb}}{2} \quad \text{(40)}$$

Here, $\langle\alpha_L\rangle_r$ is also given by Eq. 23, where the mass of the liquid phase in the riser is always positive, $(m_L)_r \geq 0$, which makes $(\alpha_L)_r \geq 0$. $(\alpha_L)_{rb}$ is determined by the flow area of the liquid phase at the riser base (low point) as $(\alpha_L)_{rb} = A_L/A_p$. Therefore, the liquid volume fraction at the top of the riser becomes

$$(\alpha_L)_{rt} = 2\langle\alpha_L\rangle_r - (\alpha_L)_{rb} = \frac{2(m_L)_r}{V_r\rho_L} - \frac{A_L}{A_p}, \quad \text{(41)}$$

We consider the lower and upper limits $\langle\alpha_L\rangle_r \geq (\alpha_L)_{rt} \geq 0$, and we use in the model

$$(\alpha_L)_{rt} = \begin{cases} \langle\alpha_L\rangle_r, & \text{if } (\alpha_L)_{rb} \leq \langle\alpha_L\rangle_r; \\ 2\langle\alpha_L\rangle_r - (\alpha_L)_{rb}, & \text{if } \langle\alpha_L\rangle_r < (\alpha_L)_{rb} < 2\langle\alpha_L\rangle \\ 0, & \text{if } (\alpha_L)_{rb} \geq 2\langle\alpha_L\rangle_r. \end{cases} \quad \text{(42)}$$

Implementation of the Model. The model equations have been implemented and solved with MATLAB. The MATLAB codes for the models are available at the homepage of Sigurd Skogestad (Jahanshahi 2012).

Comparison of the Models

OLGA Test Case and Reference Model. To study the dominant dynamic behavior of a typical (yet simple) riser slugging problem, we consider the test case for severe slugging used in the OLGA simulator. The geometry of the system is given in **Fig. 5.** The pipeline diameter is 0.12 m and its length is 4300 m. Starting from the inlet, the first 2000 m of the pipeline is horizontal and the remaining 2300 m inclines downward with a 1° angle. This gives rise to a 40.14-m descent and creates a low point at the end of the pipeline. The riser is a vertical 300-m pipe with a diameter of 0.1 m. A 100-m horizontal section with the same diameter as that of the riser connects the riser to the outlet choke valve. The feed into the system is nominally constant at 9 kg/s, with $(w_L)_{\text{in}}$=8.64 kg/s (oil) and $(w_G)_{\text{in}}$=0.36 kg/s (gas). The separator pressure (P_s) after the choke valve is nominally constant at 50.1 bar. This leaves the choke valve opening (Z_1) as the only operationally realistic control variable in the system. The model constants for the OLGA case are given in **Table 1.**

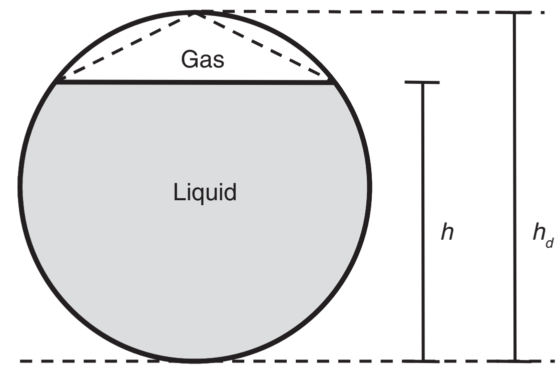

Fig. 4—Cross section of pipe at low point.

For the present case study, the critical value of the relative valve opening for the transition between a stable nonoscillatory flow regime and riser slugging is $Z_1^* = 5\%$. The superscript * is used to define the critical values of the relative valve opening. The transition between the two flow regimes is illustrated by the OLGA simulations in **Fig. 6,** which shows the inlet pressure, topside pressure, and outlet flow rate, with the valve openings of 4% (no slug), 5% (transient), and 6% (riser slugging).

Model Fitting. The six different simplified models were simulated in MATLAB, and their tuning parameters were adjusted to match the OLGA reference-model simulations. We believe that the obtained tuning parameters for all the models result in the best possible fit. The four main tuning parameters for the new pipeline/riser model are

- K_h: correction factor for the level of liquid in pipeline (Eq. 10)
- C_{v1}: production choke valve constant (Eq. 2)
- K_G: coefficient for gas flow through the low point (Eq. 32)
- K_L: coefficient for liquid flow through the low point (Eq. 37)

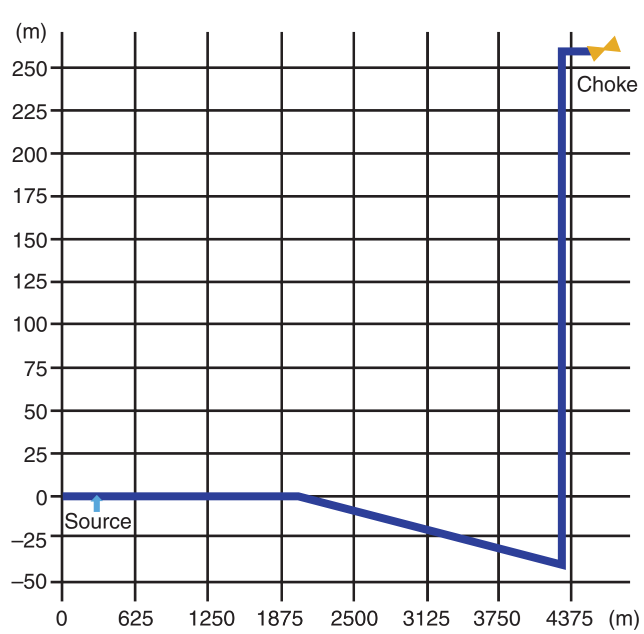

Fig. 5—Geometry of OLGA pipeline/riser test case.

Symbol	Description	Value	Unit
R	Universal gas constant	8314	J/(kmol·K)
g	Gravity	9.81	m/s^2
μ_L	Liquid viscosity	1.43×10^{-4}	Pa·s
μ_G	Gas viscosity	1.39×10^{-5}	Pa·s
ε	Pipe roughness	2.80×10^{-5}	m
ρ_L	Liquid density	832.2	kg/m^3
M_G	Gas molecular weight	20	g
T_p	Pipeline temperature	337	°K
V_p	Pipeline volume	48.63	m^3
D_p	Pipeline diameter	0.12	m
L_p	Pipeline length	4300	m
T_r	Riser temperature	298.3	°K
V_r	Riser volume	3.14	m^3
D_r	Riser diameter	0.1	m
L_r	Riser length	300	m
L_h	Length of horizontal section	100	m
P_s	Separator pressure	50.1	bar
$(\omega_L)_{in}$	Inlet liquid mass flow	8.64	kg/s
$(\omega_G)_{in}$	Inlet gas mass flow	0.36	kg/s

Table 1—Model constants for pipeline/riser OLGA case.

The tuning parameters can be adjusted to fit the model to numerical data from a given pipeline/riser system. The numerical data can be from the historical database of the oil field, from experiments, or from simulating a detailed model of the system (e.g., OLGA simulator).

To find the tuning parameters, the obvious approach is to formulate an optimization problem and to use an optimization routine in MATLAB [e.g., fmincon( )] to solve it. However, the multiobjective nature of the problem, as mentioned in the Introduction, makes it difficult to formulate and solve such an optimization problem. Thus, we decided to use a simpler approach.

We performed the model fitting by trying to match the essential features of the simulated results from OLGA. First, we simulated the OLGA reference model for a nonslug operating point $\left(Z_1 < Z_1^*\right)$, and we recorded the pipeline inlet pressure P_{in}, the riser top pressure P_{rt}, the inlet liquid mass flow $(w_L)_{in}$, the inlet gas mass flow $(w_G)_{in}$, and the valve opening Z_1. From these five values, we back calculated to $(\rho_G)_p$, ΔP_G, ΔP_L, and ρ_{rt} on the basis of the model equations. Finally, by inverting Eqs. 32, 37, and 2, we obtained

$$K_G = \frac{\gamma_1 \left(w_G\right)_{in}}{A_G \sqrt{\left(\rho_G\right)_p \Delta P_G}}, \qquad (43)$$

$$K_L = \frac{\gamma_2 \left(w_L\right)_{in}}{A_L \sqrt{\rho_L \Delta P_L}}, \qquad (44)$$

and

$$C_{v1} = \frac{\gamma_3 \left[\left(w_G\right)_{in} + \left(w_L\right)_{in}\right]}{Z_1 \sqrt{\rho_{rt} \max\left(P_{rt} - P_s, 0\right)}}, \qquad (45)$$

where $0.5<\gamma_1<2$, $0.5<\gamma_2<2$, and $0.8<\gamma_3<1.2$ are dimensionless coefficients used to fine tune the model manually. These γ values are expected to be equal to unity; however, they must be changed to obtain a good fit. The complete set of equations for this procedure is given in the MATLAB code provided online (Jahanshahi 2012). The

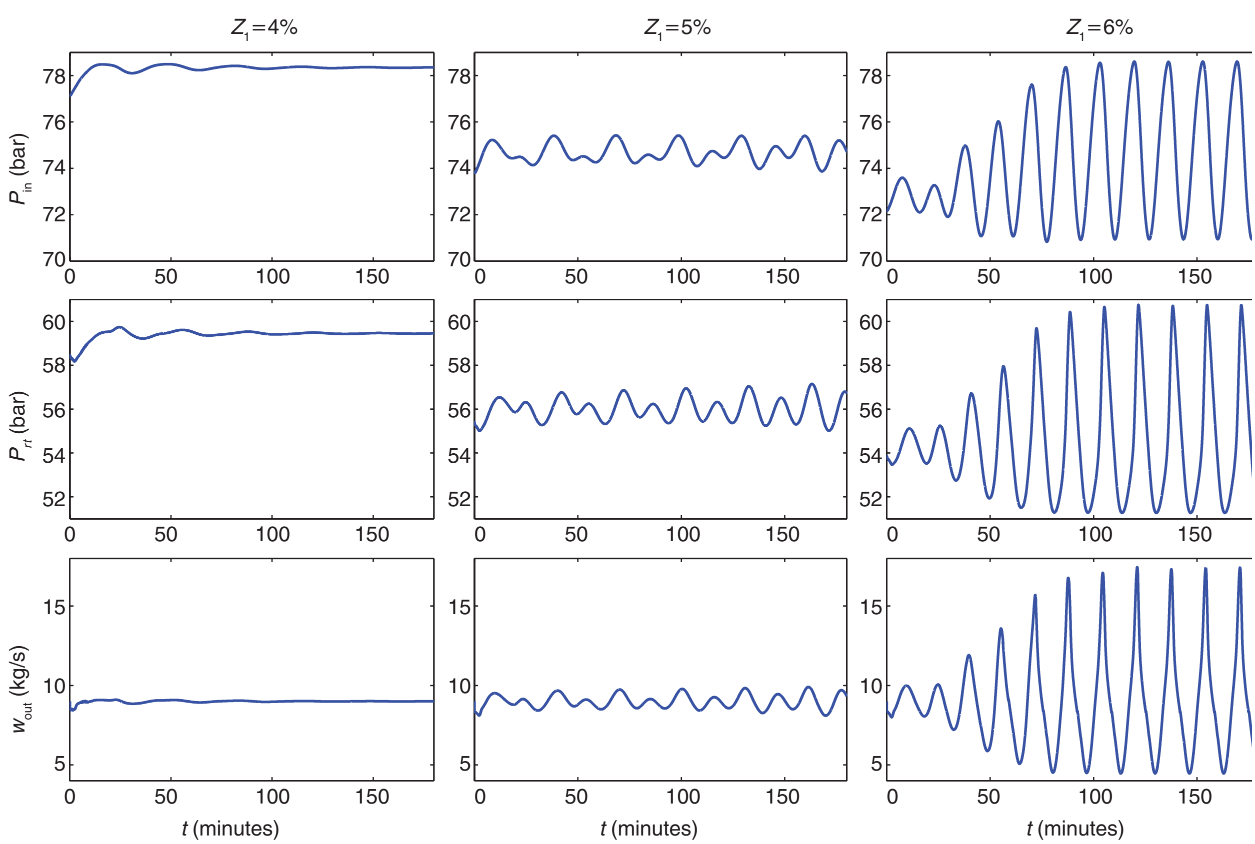

Fig. 6—Simulations of OLGA test case for different valve openings.

Symbol	Description	Value
K_h (–)	Correction factor for the level of liquid in the pipeline	0.700
K_G (–)	Coefficient for gas flow through the low point	3.87×10^{-2}
K_L (–)	Coefficient for liquid flow through the low point	1.64×10^{-1}
C_{v1} (m^2)	Production choke valve constant	1.12×10^{-2}

Table 2—Tuning parameters for pipeline/riser model fitted to OLGA simulations.

fourth tuning parameter $K_h \approx 1$ was found by trial and error. For the OLGA case, we found $K_h = 0.7$, and for the experiments it was exactly 1.0. By this approach, we always obtain parameter values that give a single, physically meaningful solution to the model. The four main tuning parameters of the new model fitted to the OLGA case are given in **Table 2.**

A similar systematic approach has been proposed by Di Meglio et al. (2010) for tuning the Di Meglio model, but this tuning procedure did not work well for the present case study. The Di Meglio model includes five tuning parameters (C_c, C_g, ε, V_{eb}, and m_{still}). The Di Meglio tuning procedure finds four of the parameters; it does not give the value of C_g, which must be found by trial and error. We tried the tuning procedure by Di Meglio et al. (2010), and the obtained values are listed in **Table 3.** However, these values do not produce a good match; we had to change the three first parameters in Table 3 to obtain a good fit. Note that the case study considered by Di Meglio et al. (2010) is different from the OLGA case used in this work; their system does not include the low point and the horizontal pipe. This may be the reason that their tuning procedure did not work for the present case study.

Comparison of the Models With the OLGA Simulations. The results for the six models are summarized in **Table 4,** which shows the error of various model-fitting criteria. The error percentage for each quantity X is shown inside the parentheses and is calculated as $Error\ \% = \text{abs}\left(\frac{X_{\text{model}}}{X_{\text{OLGA}}} - 1\right) \times 100$. The most important criterion for the model fitting is the critical value of the valve opening (Z_1^*), and all the models were adjusted to match this value. Next, we looked at the oscillation frequency at this point (T_c), which could not be matched exactly by the Eikrem and Nydal models. For the present case study, we obtained $Z_1^* = 5\%$ and $T_c = 15.6$ minutes from simulations performed with OLGA version 5.3.

Frequency of Oscillations. All models were linearized at the critical operating point, $Z_1^* = 5\%$. The period of oscillations at this operating point is directly related to the poles of the linear models. Most of the models give a pair of complex conjugate poles, $s = \pm\omega_c i = \pm 0.0067i$. Note that the critical frequency is $\omega_c = \frac{2\pi}{T_c} = \frac{2\pi}{15.6(\text{minutes})60(\text{s/min})} = 0.0067\ \text{s}^{-1}$. The exceptions are the Eikrem and Nydal models, which are not able to obtain the correct period time (15.6 minutes), and consequently they result in different poles at $Z_1^* = 5\%$.

Step Response. **Fig. 7** shows the pressure response at the top of the riser to a step change in the valve opening from $Z_1 = 4\%$ to $Z_1 = 4.2\%$ for the OLGA reference model and the new model. The step response of the OLGA model has one undershoot and one overshoot. The amplitudes of the overshoot and undershoot for different simplified models are given in Table 4 in the form of errors from those of the OLGA model.

The inverse response (overshoot) corresponds to the right-half-plane zeroes near the imaginary axis, which are also given for $Z_1 = 5\%$ in Table 4. Note that the poles and the zeroes are related to frequencies of the transfer functions (Laplace transform), which are complex numbers in general, and i in the table shows the imaginary part.

Bifurcation Diagrams. Similar to the simulations shown in Fig. 6, we simulate the models for different valve openings, covering the entire operational range of the valve, to obtain the bifurcation diagrams as shown in **Fig. 8.** Bifurcation diagrams demonstrate the transition from nonslug to slugging flow at the critical valve opening if the system is not controlled (i.e., when the valve opening is manually set to constant values). For $Z_1 > 5\%$, the steady-state (nonslug) flow regime shown by the central line does not exist normally, because it is an unstable equilibrium for the system, but it can be stabilized with feedback control [like an inverted pendulum, which is a standard example in nonlinear control textbooks (e.g., Khalil 2002)][1]. The nonslug behavior of the new model and also the minimum and maximum of the oscillations are compared with those of the OLGA model in Fig. 8. To have a quantitative comparison, deviations of the different simplified models from the OLGA reference model for a fully open valve ($Z_1 = 100\%$) are summarized in Table 4. Among the simplified models, the new model retains the best fit to the bifurcation diagrams; the second-best fit was obtained with the Di Meglio model, as shown in **Fig. 9.**

Note that because we want to use control to avoid slugging, the nonslug behavior is much more important for control purposes than the minimum and maximum oscillatory (slugging) pressure values. Another analogy is riding a bicycle and the need to keep it upright (nonslug), which is otherwise a naturally unstable position. If the bicycle falls down to the ground (slug), it is too late to control it. Hence, a model for the fallen bicycle (slug) is not useful for control.

Comparison Summary. As seen in Table 4, there is a trade-off between model "complexity" and the number of tuning parameters used to match the actual process data. Here, the term complexity, as used in Table 4, is a somewhat fuzzy qualitative measure. Generally, models with a simple structure can achieve a good fit to complicated physical processes by excess use of fitting parameters. A good example from the model-fitting literature is the work of Wei (1975), which shows that by use of many fitting parameters, one can fit a simple model to match the shape of an elephant.

[1]This system has two equilibria: one stable equilibrium at $\theta = 0°$ and one unstable equilibrium at $\theta = 180°$, where the pendulum is inverted.

Symbol	Description	Values Found by Di Meglio Procedure	Values Found by Trial and Error for Good Fit
ε (–)	Split inflow of gas	1.82×10^{-2}	3.50×10^{-1}
V_{eb} (m^3)	Volume of gas in the pipeline	1.25×10^{1}	1.16×10^{1}
$m_{l,\text{still}}$ (kg)	Still mass of liquid in riser	4.89×10^{2}	0
C_g (–)	Coefficient of gas flow through virtual valve	2.57×10^{-5}	2.57×10^{-5}
C_c (m^2)	Production choke valve constant	2.56×10^{-1}	2.56×10^{-1}

Table 3—Tuning parameters for the model by Di Meglio et al. (2010).

Parameters	OLGA Simulation	Storkaas Model	Eikrem Model	Kaasa Model	Nydal Model	Di Meglio Model	New Model
State equations	Many	3 differential, 1 algebraic	4 differential	3 differential	4 differential	4 differential	4 differential
Model complexity	Complicated	Average	Simple	Very simple	Average	Simple	Average
Tuning parameters	—	5	3	7	3	5	4
Right-half-plane zeroes of P_{rt} at Z = 5%	—	0.0146	0.006+0.005*i* 0.006–0.005*i*	—	0.0046	0.019+0.034*i* 0.019–0.034*i*	0.0413 0.0126
Values From OLGA Simulator		**Error of Simplified Models When Compared With OLGA**					
Critical valve opening	5%	0 (0%)	0 (0%)	0 (0%)	0 (0%)	0 (0%)	0 (0%)
Period (minutes) at Z = 5%	15.6	0 (0%)	26.15 (168%)	0 (0%)	15.97 (102%)	0 (0%)	0 (0%)
Step response of P_{rt}							
Undershoot	–0.098	0.10 (99%)	0.08 (78%)	—	0.12 (89%)	0.07 (68%)	0.05 (54%)
Overshoot	0.198	0.16 (80%)	0.18 (89%)	—	0.10 (50%)	0.17 (84%)	0.10 (51%)
At t = 10 minutes	–0.824	0.43 (53%)	0.62 (75%)	—	0.25 (30%)	0.47 (58%)	0.33 (41%)
Steady state							
P_{in} (bar)	68.22	1.9 (2.7%)	4.4 (6.46%)	—	1.77 (2.6%)	0.71 (1%)	0.21 (0.32%)
P_{rb} (bar)	66.76	—	—	0.02 (0.04%)	—	—	—
P_{rt} (bar)	50.10	0.01 (0.02%)	0.01 (0.02%)	—	0.01 (0.02%)	0.01 (0.02%)	0.01 (0.02%)
ω_{out} (kg/s)	9.00	0 (0%)	0 (0%)	—	2.90 (32%)	0 (0%)	0 (0%)
Minimum							
P_{in} (bar)	63.50	2.7 (4.3%)	9 (14.2%)	—	8.3 (13%)	2.6 (4.1%)	2.0 (3.1%)
P_{rb} (bar)	62.08	—	—	2.57 (4.1%)	—	—	—
P_{rt} (bar)	50.09	$4{\times}10^{-4}$ ($8{\times}10^{-4}$%)	$5{\times}10^{-4}$ ($9{\times}10^{-4}$%)	—	0.41 (0.82%)	0.003 (0.006%)	$4{\times}10^{-4}$ ($8{\times}10^{-4}$%)
ω_{out} (kg/s)	0.791	0.55 (69%)	0.14 (17%)	—	0.79 (100%)	3.3 (405%)	0.55 (69%)
Maximum							
P_{in} (bar)	75.83	1.4 (1.8%)	1.89 (2.5%)	—	1.00 (1.3%)	1.3 (1.7%)	1.9 (2.6%)
P_{rb} (bar)	74.55	—	—	0.55 (0.075%)	—	—	—
P_{rt} (bar)	50.14	1.5 (3%)	0.95 (1.9%)	—	1.09 (2.2%)	0.71 (0.35%)	0.1 (0.2%)
ω_{out} (kg/s)	31.18	80 (278%)	57 (200%)	—	13.3 (43%)	22 (77%)	2.0 (7.0%)

Table 4—Comparison of different simplified models with the OLGA reference case.

Here, simple models, such as those of Kaasa and Di Meglio, use seven and five tuning parameters, respectively, to get a good fit. However, finding the parameter values for these models is not easy and straightforward. The Nydal model and the Eikrem model (with three parameters) are also simple, but they are not able to match the OLGA simulations because of too few tuning parameters. The new model (with four parameters) is somewhat more complicated, but is able to give a reasonable match with relatively few tuning parameters. Also, as opposed to the other simplified models, the new model does not require adjusting any physical property of the system, such as volume of gas in the pipeline.

The new model and the De Meglio model show similar accuracy in prediction of the steady state and the minimum and maximum values, but dynamically, the new model is closer to the OLGA simulations.

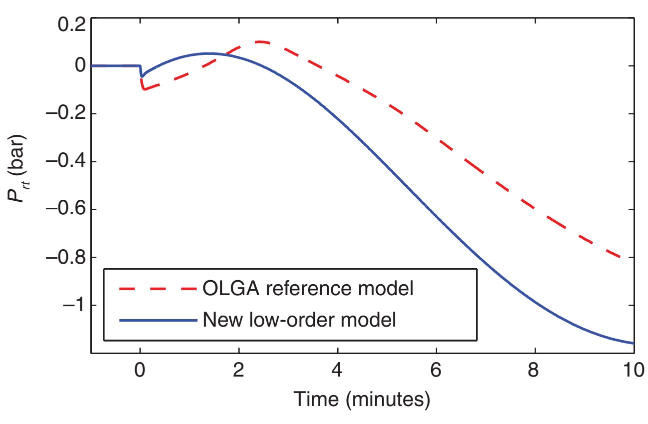

Fig. 7—Response of pressure at the top of the riser to a step change in the valve opening from Z_1=4% to Z_1=4.2% for the OLGA reference model (dashed line) and the new model (solid line).

Comparison With Experiments. The experiments were performed on a laboratory setup for antislug control at the Chemical Engineering Department of the Norwegian University of Science and Technology. **Fig. 10** shows a schematic of the laboratory setup. The pipeline and the riser are made from flexible pipes with a 2-cm inner diameter. The length of the pipeline is 4 m, and it is inclined with a 15° angle. The height of the riser is 3 m. A buffer tank is used to simulate the effect of a long pipe with the same volume, such that the total resulting length of pipe would be approximately 70 m. Other model constants are given in **Table 5,** and the four tuning parameters of the model fitted to the experiments are given in **Table 6.** The topside choke valve is used as the input for control. The separator pressure after the topside choke valve is nominally constant at atmospheric pressure. The feed into the pipeline is assumed to be at constant flow rates, 4

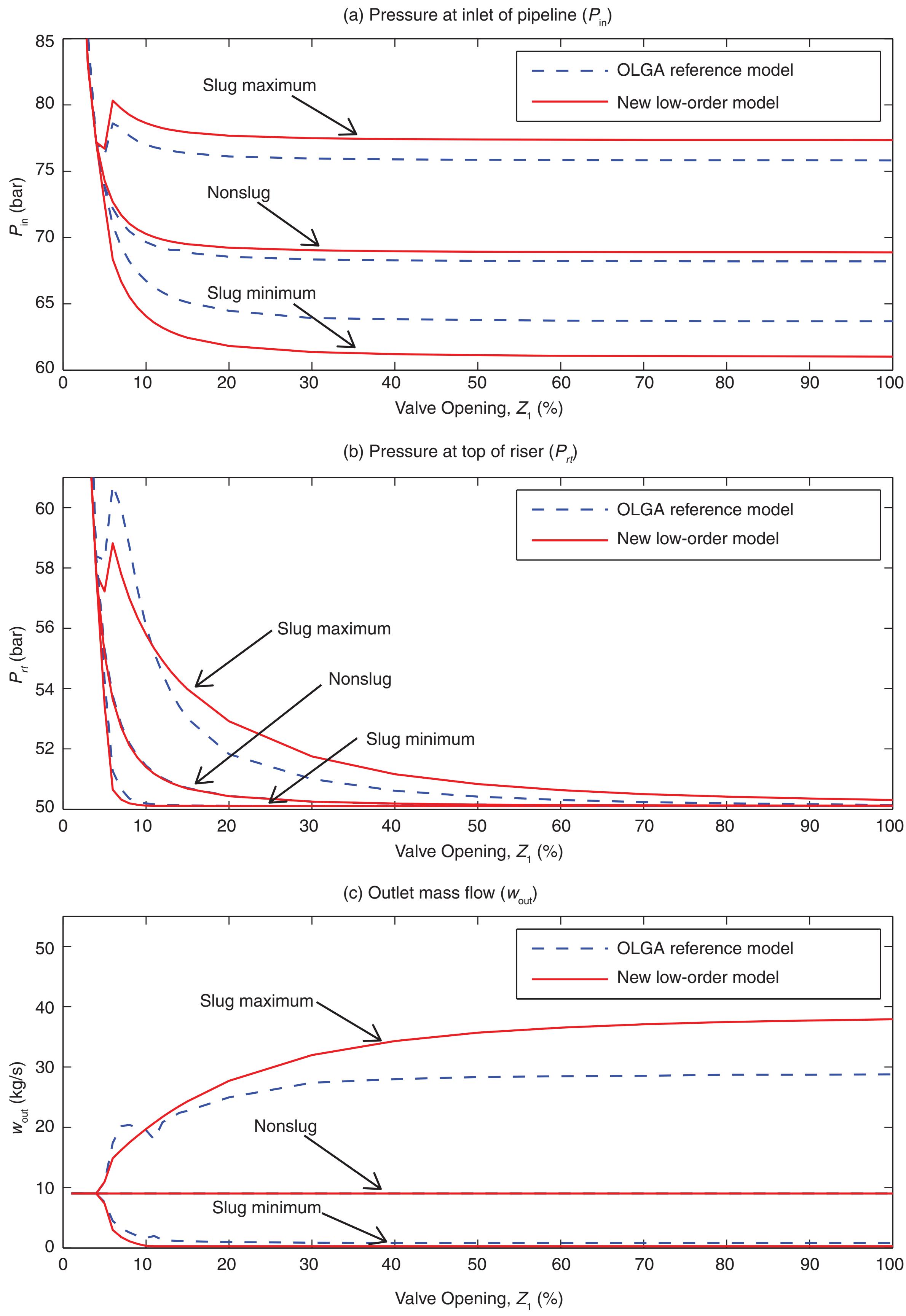

Fig. 8—Bifurcation diagrams of new simplified pipeline/riser model (solid lines) compared with the OLGA reference model (dashed). At small valve openings (Z_1<5%), there is no slugging. At large valve openings, slugging occurs and the two additional curves give the maximum and minimum of the oscillations. The intermediate steady-sate (i.e., nonslug) condition can be maintained with feedback control.

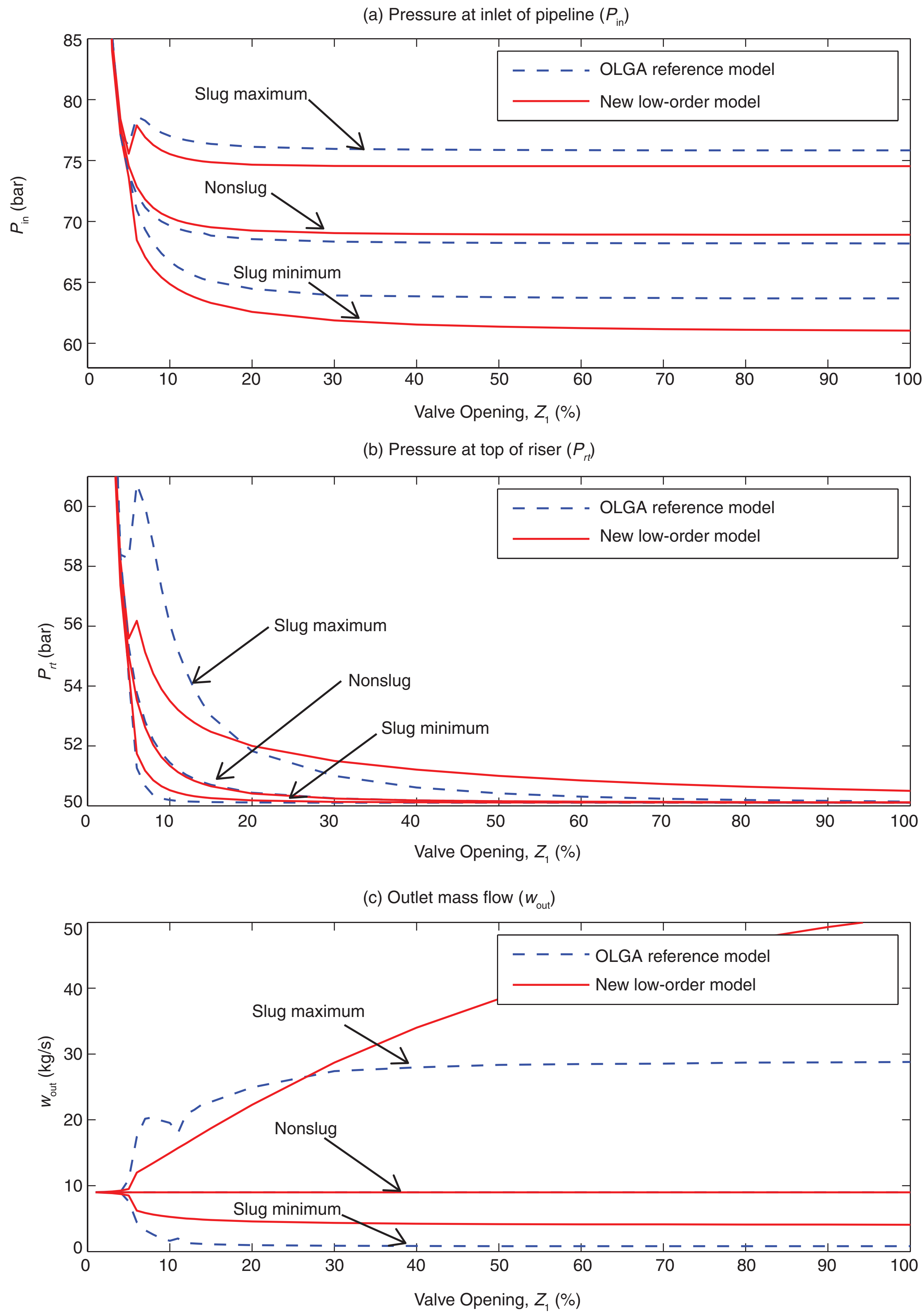

Fig. 9—Bifurcation diagrams of Di Meglio pipeline/riser model (solid lines) compared with the OLGA reference model (dashed).

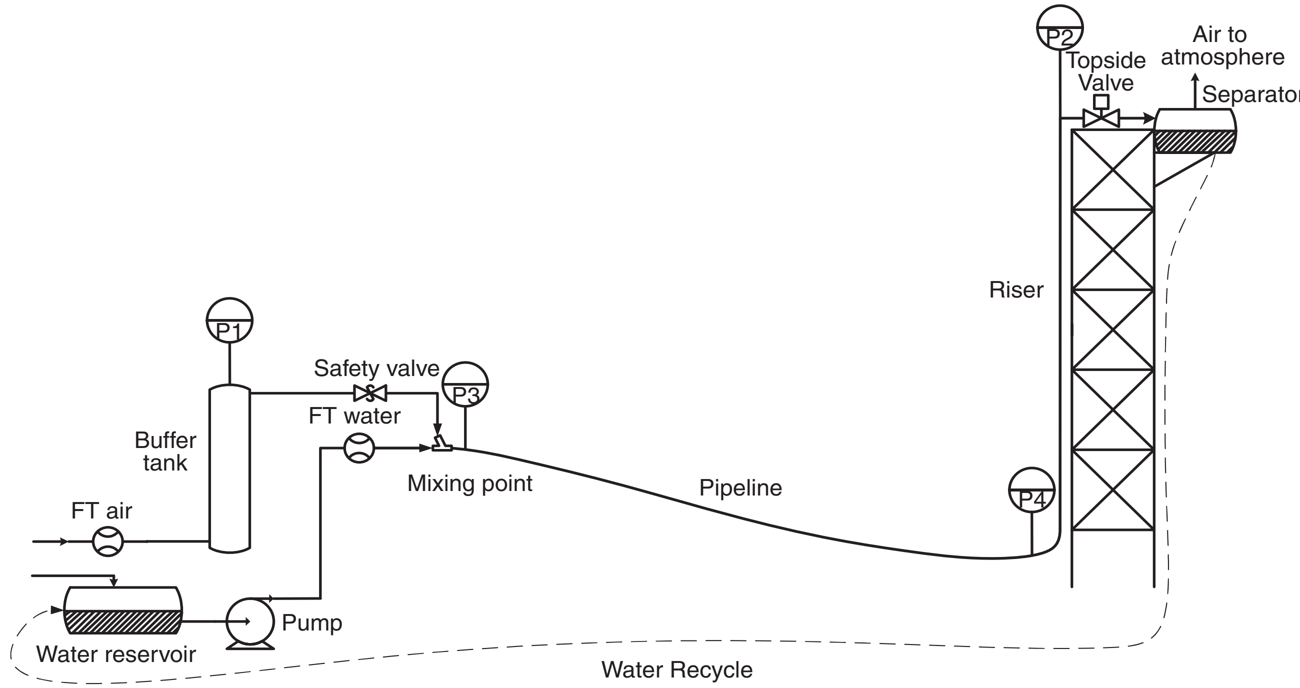

Fig. 10—Experimental setup.

Symbol	Description	Value	Unit
μ_L	Liquid viscosity	8.90×10^{-4}	Pa·s
μ_G	Gas viscosity	1.81×10^{-5}	Pa·s
ε	Pipe roughness	1.00×10^{-6}	m
ρ_L	Liquid density	1000	kg/m^3
M_G	Gas molecular weight	18	g
T_p	Pipeline temperature	288	K
V_p	Pipeline volume	0.0219	m^3
D_p	Pipeline diameter	0.02	m
L_p	Pipeline length	69.71	m
T_r	Riser temperature	288	K
V_r	Riser volume	0.001	m^3
D_r	Riser diameter	0.02	m
L_r	Riser length	3	m
L_h	Length of horizontal section	0.2	m
P_s	Separator pressure	1.013	bar

Table 5—Model constants for small-scale experimental setup.

L/min of water and 4.5 L/min of air. With these boundary conditions, the critical valve opening at which the system switches from stable (nonslug) to oscillatory (slug) flow is $Z_1^*=15\%$.

In addition, we developed a new OLGA case with the same dimensions and boundary conditions as those of the experimental setup. The bifurcation diagrams are shown in **Fig. 11,** where the simplified model (thin solid lines) is compared with the experiments (bold solid lines) and the OLGA model (dashed lines). In Fig, 11, the system has a stable (nonslug) flow when the topside valve opening Z_1 is smaller than 15%, and it switches to slugging flow conditions for $Z_1>15\%$.

Well/Pipeline/Riser System

In the pipeline/riser model described in the preceding, constant gas- and liquid-flow rate were used as inlet boundary conditions. In order

K_h (–)	Correction factor for level of liquid in pipeline	1.00
K_G (–)	Coefficient for gas flow through low point	1.42×10^{-2}
K_L (–)	Coefficient for liquid flow through low point	1.90×10^{-1}
C_{v1} (m^2)	Production choke valve constant	2.39×10^{-4}

Table 6—Tuning parameters for pipeline/riser model fitted to experiments.

to study the effect the of pressure-induced (pressure-governed) inflow, which is more physically realistic, we add an oil well and assume a constant reservoir pressure as the boundary condition (see **Fig. 12**).

Simplified Six-State Model. We add two state variables—the mass of gas and mass of liquid inside the oil well—to the pipeline/riser system in Eqs. 1a through 1d to obtain a six-state model. The two additional state equations are

$$\frac{\mathrm{d}(m_G)_w}{\mathrm{d}t}=\left(\frac{\eta}{\eta+1}\right)w_r-(w_G)_{wh} \quad (46)$$

and

$$\frac{\mathrm{d}(m_L)_w}{\mathrm{d}t}=\left(\frac{1}{\eta+1}\right)w_r-(w_L)_{wh}\ , \quad (47)$$

where η is the average mass ratio of gas and liquid produced from the reservoir, which is assumed to be a known parameter of the well. $(w_G)_{wh}$ and $(w_L)_{wh}$ are the mass-flow rates of gas and liquid at the wellhead. The production mass rate w_r (kg/s) from the reservoir to the well is assumed to be described by a linear inflow-performance relationship,

$$w_r=C_{PI}\max\left(0,P_{\mathrm{res}}-P_{bh}\right)\ , \quad (48)$$

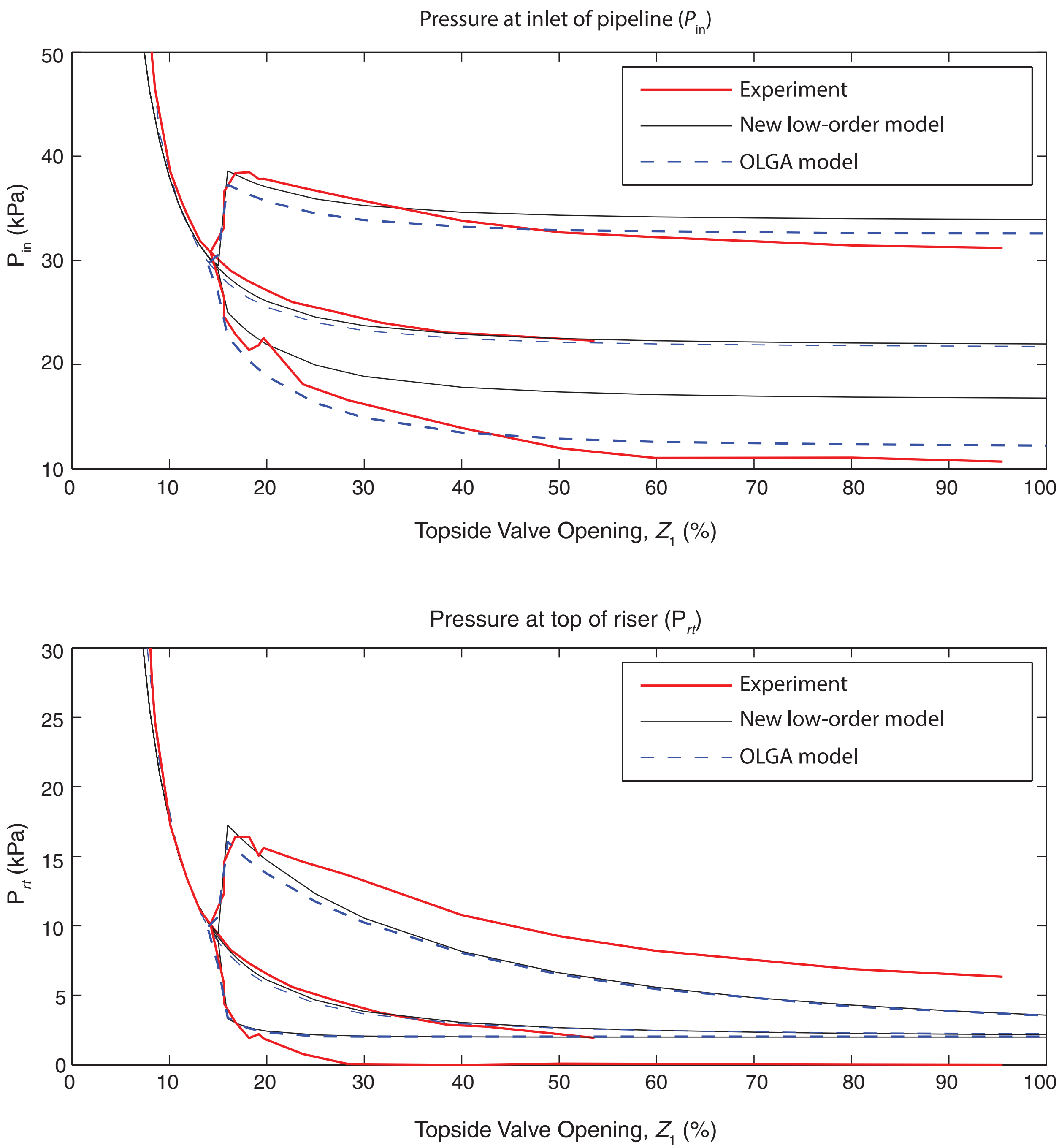

Fig. 11—Bifurcation diagrams of simplified pipeline/riser model (thin solid lines) compared with experiments (thick red solid lines) and OLGA simulations (dashed blue lines).

where C_{PI} [kg/(s·Pa)] is the mass productivity constant of the well; P_{res} is the reservoir pressure, which can be assumed constant in a short period of time (e.g., a few months); and P_{bh} is the flowing bottomhole pressure of the well,

$$P_{bh} = P_{wh} + \langle \rho_m \rangle_w gL_w + (\Delta P_f)_w \quad \text{.......(49)}$$

In Eq. 49, $(\Delta P_f)_w$ is the pressure loss because of friction in the well, which is assumed to be given as

$$(\Delta P_f)_w = \frac{\lambda_w \langle \rho_m \rangle_w \langle U_m \rangle_w^2 L_w}{2D_w} \quad \text{.......(50)}$$

We obtain λ_w, the friction factor for the flowing well, in the same manner as Eq. 26, except we replace subscript r with w (i.e., we substitute riser dimensions, mixture Reynolds number, and viscosity with parameters applicable to the wellbore).

The average liquid volume fraction inside the well is $\langle \alpha_L \rangle_w = (m_L)_w / V_w \rho_L$, and the average mixture velocity in the well is

$$\langle U_m \rangle_w = \frac{4 \langle w_{\text{nom}} \rangle}{\pi D_w^2 \langle \rho_m \rangle_w}, \quad \text{.......(51)}$$

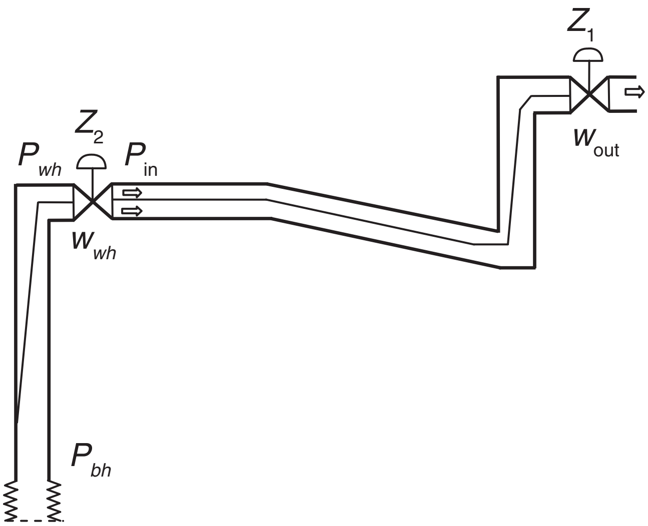

Fig. 12—Schematic of the well/pipeline/riser system.

Symbol	Description	Value	Unit
P_{res}	Reservoir pressure	320	bar
C_{PI}	Mass productivity constant	2.75×10^{-6}	kg/(s·Pa)
$\langle w_{nom} \rangle$	Well nominal mass flow	9	kg/s
η	Mass gas/oil ratio	0.04	–
T_w	Well temperature	369	K
V_w	Well volume	33.93	m^3
D_w	Well diameter	0.12	m
L_w	Well depth	3000	m
ε	Well roughness	2.80×10^{-5}	m

Table 7—Model constants for well section.

where $\langle w_{nom} \rangle$ is an a priori known nominal flow rate of the well, and the average density of the two-phase mixture is

$$\langle \rho_m \rangle_w \frac{(m_G)_w + (m_L)_w}{V_w} \quad . \qquad (52)$$

The density of the gas phase in the well is

$$\langle \rho_G \rangle_w \frac{(m_G)_w}{V_w - (m_L)_w / \rho_L} \quad , \qquad (53)$$

so the pressure at the wellhead, assuming ideal gas, becomes

$$P_{wh} = \frac{(\rho_G)_w RT_{wh}}{M_G} \quad , \qquad (54)$$

To calculate the liquid volume fractions at the top of the well, we use the same assumptions as those used for the phase fraction of the riser:

$$(\alpha_L)_{wt} = 2K_\alpha \langle \alpha_L \rangle_w - (\alpha_L)_{wb} \quad . \qquad (55)$$

In this case, because of the high pressure at the bottom of the hole, the fluid from the reservoir is saturated (Ahmed 2006) and the liquid volume fraction at the bottom is $(\alpha_L)_{wb}=1$. $K \approx 1$ is a tuning parameter that can be used for model-fitting purposes. The gas mass fraction at the top of the well is then

$$(\alpha_G^m)_{wt} = \frac{\left[1-(\alpha_L)_{wt}\right](\rho_G)_w}{(\alpha_L)_{wt}\rho_L + \left[1-(\alpha_L)_{wt}\right](\rho_G)_w} \quad . \qquad (56)$$

The density of the mixture at the top of the well is

$$\rho_{wt} = (\alpha_L)_{wt}\rho_L + \left[1-(\alpha_L)_{wt}\right](\rho_G)_w \quad . \qquad (57)$$

The mass-flow rate of the mixture at the wellhead is

$$w_{wh} = C_{v2} f(z_2) \sqrt{\rho_{wt} \max(P_{wh} - P_{in}, 0)} \quad , \qquad (58)$$

where P_{in} is the pressure at the inlet of the pipeline, which is given by Eq. 12 in the pipeline/riser model. The flow rates of gas and the liquid phases from the wellhead are as follows:

$$(w_G)_{wh} = (\alpha_G^m)_{wt} w_{wh} \qquad (59)$$

and

$$(w_L)_{wh} = \left[1-(\alpha_G^m)_{wt}\right] w_{wh} \quad . \qquad (60)$$

Flow rates of gas and liquid phases into the pipeline are, respectively,

$$(w_G)_{in} = (w_G)_{wh} + d_1 \qquad (61)$$

and

$$(w_L)_{in} = (w_L)_{wh} + d_2 \quad , \qquad (62)$$

where d_1 and d_2 are assumed to represent disturbances on feed flow rates from the other production wells in the network. Usually, multiple production wells are connected to a subsea manifold, and their products are combined and transported through a shared pipeline. In this paper, we have considered only one oil well. This can be easily extended for multiple oil wells in a network.

For the nominal case, d_1 and d_2 are zero. Generally, d_1 and d_2 are zero-mean random variables and their maximum values are assumed to be 10% of $(w_G)_{wh}$ and $(w_L)_{wh}$, respectively. The role of the disturbances is very important when the model is used for control and optimization applications. The feedback controller and the optimizer are usually designed on the basis of a nominal model (without disturbances), but they need to be robust against disturbances and model uncertainties.

Comparison With OLGA Simulations. In the OLGA reference-test case introduced previously, constant inflow rates were assumed. We modified the OLGA reference model by connecting an oil well to the inlet of the pipeline, as shown in Fig. 12. The oil well is vertical, has a depth of 3000 m, and it has the same inner diameter as for the pipeline (0.12 m). The reservoir pressure is constant at 230 bar. The parameters related to the pipeline and the riser are the same as those for the OLGA reference model. The constants related to the additional well section are given in **Table 7.**

The well/pipeline/riser model includes two additional tuning parameters: C_{v2}, the valve constant of the subsea choke valve, and K in Eq. 55. Hence, we have six tuning parameters in the simple well/pipeline/riser model. Numerical values for the tuning parameters are given in **Table 8.** The resulting bifurcation diagrams of the simple model are compared with the modified OLGA model in **Fig. 13.** The simple model could predict the steady state and the bifurcation point with a good accuracy. Fig. 13b shows that the inlet mass flow is increasing by opening the topside choke valve. This is because of the pressure-driven nature of the flow.

Symbol	Description	Value
K_h (–)	Correction factor for level of liquid in pipeline	0.60
K_G (–)	Coefficient for gas flow through low point	3.49×10^{-2}
K_L (–)	Coefficient for liquid flow through low point	6.55×10^{-1}
C_{v1} (m^2)	Production choke valve constant	1.26×10^{-2}
K_α (–)	Liquid fraction correction factor	0.96
C_{v2} (m^2)	Wellhead choke valve constant	3.30×10^{-3}

Table 8—Tuning parameters for well/pipeline/riser model fitted to OLGA simulations.

Conclusions

In this paper, we have derived a new, simplified dynamic model for describing severe slugging in pipeline/riser systems. Importantly, the model also predicts the nonslug-flow regime, which exists at conditions with large valve openings where slug flow occurs naturally. This nonslug regime can be obtained by applying feedback control only; for example, by adjusting the topside valve to control the riser-bottom pressure (Fig. 1).

The model is based on simple mass balances for the riser and pipeline (Fig. 2) and results in four ordinary-differential equations. In addition, models are required for the pressure drop over the pipeline and inlet of the riser (frictional pressure drop), in the riser (gravity and frictional pressure drops), and for the valve at the top of the riser (frictional pressure drop). Further, we need to determine the flow conditions at the low point and the phase distribution at the top of the riser.

We have explained how the four adjustable parameters in this model can be obtained by matching results from the much-more-detailed OLGA model (Table 2) or to experimental data (Table 6). For the OLGA pipeline/riser test case (Fig. 5), the agreement between the new simple model and the OLGA simulations is good (Figs. 7 and 8). The simple model also matches very well with the experimental results from a small-scale experimental rig (Figs. 10 and 11).

The new model incorporates features of several previously published models, and we provide in Table 4 a detailed comparison with five other simplified models (the Storkaas, Eikrem, Kaasa, Nydal, and Di Meglio models). Our new model provides the best fit, especially when taking into account that it only contains four adjustable parameters. The second-best fit is obtained with the Di Meglio model.

At the end of the paper, we show how the model can be easily extended to include other geometries—for example, with a well before the pipeline. In this case, we also obtain a very good match to OLGA simulations.

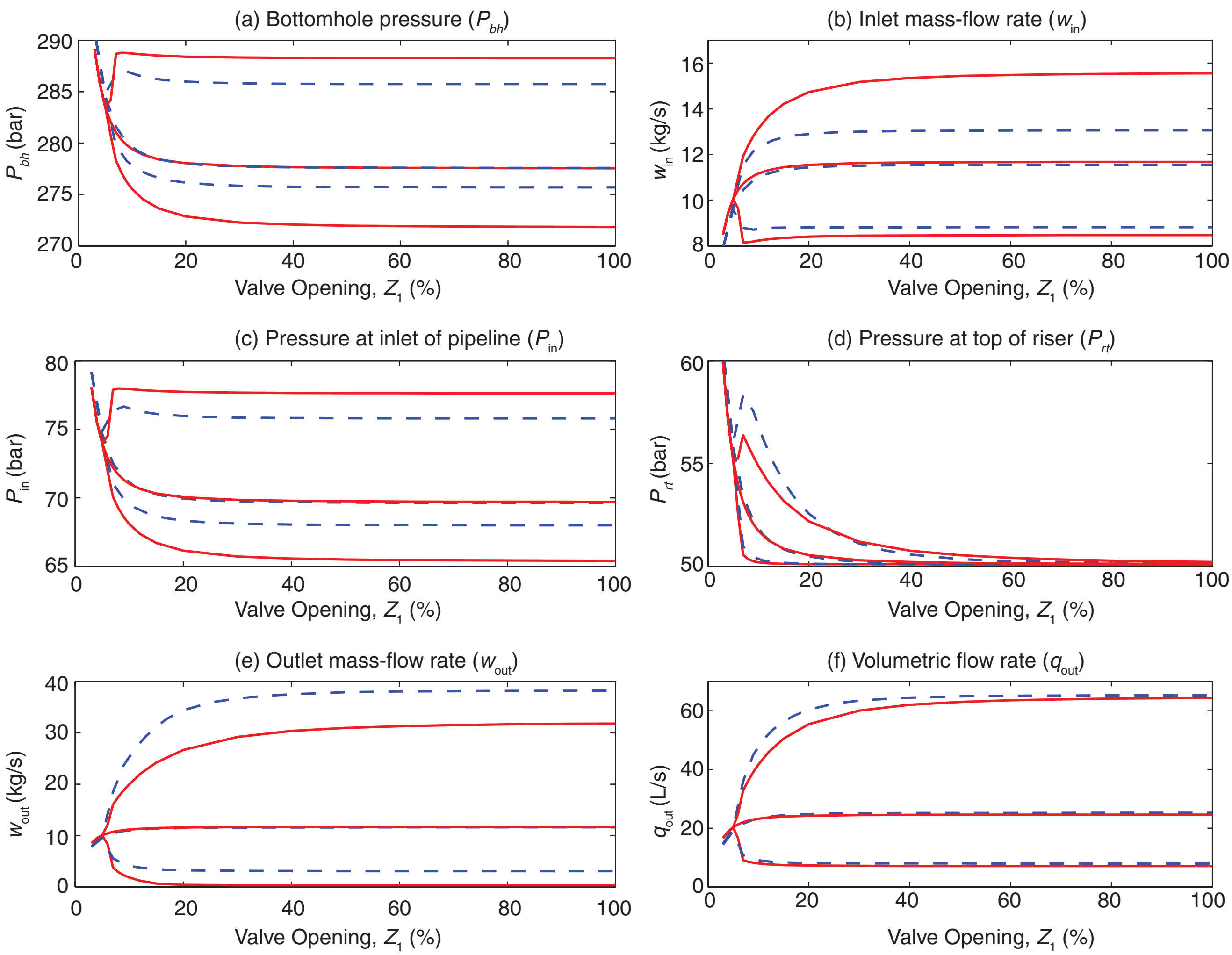

Fig. 13—Bifurcation diagrams of simplified well/pipeline/riser model (solid lines) compared with the OLGA reference model (dashed lines).

Nomenclature

Constants.

A_p = cross-sectional area of the pipeline, m^2
A_r = cross-sectional area of the riser, m^2
C_{PI} = mass productivity constant, kg/(s·Pa)
C_{v1} = production choke valve constant, m^2
C_{v2} = wellhead choke valve constant, m^2
D_p = pipeline diameter, m
D_r = riser diameter, m
D_w = well diameter, m
g = gravity, m/s^2
h_d = opening of the pipeline at the riser base, m
K_G = coefficient for gas flow through the low point, –
K_h = correction factor for level of liquid in pipeline, –
K_L = coefficient for liquid flow through the low point, –
K_α = liquid fraction correction factor, –
L_h = length of the horizontal section, m
L_p = pipeline length, m
L_r = riser length, m
L_w = well depth, m
M_G = gas molecular weight, g
P_{res} = reservoir pressure, bar
P_s = separator pressure, bar
P_{set} = pressure set point, Pa
R = universal gas constant, J/(kmol·K)
T_p = pipeline temperature, K
T_r = riser temperature, K
T_{wh} = well temperature, K
V_p = pipeline volume, m^3
V_r = riser volume, m^3
V_w = well volume, m^3
$(w_G)_{in}$ = inlet gas mass flow, kg/s
$(w_L)_{in}$ = inlet liquid mass flow, kg/s
$\langle w_{nom} \rangle$ = well nominal mass flow, kg/s
Z_1^* = critical value of the valve opening, %
ε = pipe roughness, m
η = gas/oil mass ratio, –
μ_G = gas viscosity, Pa·s
μ_L = liquid viscosity, Pa·s
ρ_G = gas density, kg/m^3
ρ_L = liquid density, kg/m^3

Variables.

A_G = free area for gas flow at the low point, m^2
A_L = area for liquid flow at the low point, m^2
d_1 = disturbance on inflow of gas to the pipeline, kg/s
d_2 = disturbance on inflow of liquid to the pipeline, kg/s
h = level of liquid in the pipeline, m
$\langle h \rangle$ = average level of liquid at the low point, m
$(m_G)_p$ = mass of gas in the pipeline, kg
$(m_G)_r$ = mass of gas in the riser, kg
$(m_G)_w$ = mass of gas in the well, kg
$(m_L)_p$ = mass of liquid in the pipeline, kg
$(m_L)_r$ = mass of liquid in the riser, kg
$(m_L)_w$ = mass of liquid in the well, kg
$\langle m_L \rangle_p$ = average mass of the liquid in the pipeline, kg
$(N_{Re})_p$ = Reynolds number of flow in the pipeline, –
$(N_{Re})_r$ = Reynolds number of flow in the riser, –
P_{bh} = flowing bottomhole pressure, Pa
P_{in} = pressure at the inlet of the pipeline, Pa
$P_{in,nom}$ = nominal (steady-state) pressure at the pipeline inlet, Pa
P_{rt} = pressure at the top of the riser, Pa
P_{wh} = wellhead pressure, Pa
q_{out} = volumetric rate of outflow, m^3/s
T_c = oscillation frequency, minutes
$\langle U_m \rangle_p$ = average mixture velocity in the pipeline, m/s
$\langle U_m \rangle_r$ = average mixture velocity in the riser, m/s
$\langle U_m \rangle_w$ = average mixture velocity in the well, m/s
$\langle U_{sG} \rangle_p$ = average superficial velocity of gas in the pipeline, m/s
$\langle U_{sG} \rangle_r$ = average superficial velocity of gas in the riser, m/s
$\langle U_{sL} \rangle_p$ = average superficial velocity of liquid in the pipeline, m/s
$\langle U_{sL} \rangle_r$ = average superficial velocity of liquid in the riser, m/s
$(V_G)_p$ = volume of gas in the pipeline, m^3
$(V_G)_r$ = volume of gas in the riser, m^3
w_{out} = mass-flow rate of outlet mixture, kg/s
w_r = production mass rate from the reservoir, kg/s
w_{wh} = mass-flow rate of the mixture at the wellhead, kg/s
$(w_G)_{out}$ = mass-flow rate of outlet gas, kg/s
$(w_G)_{rb}$ = mass-flow rate of gas at the riser base, kg/s
$(w_G)_{wh}$ = mass-flow rate of gas at the wellhead, kg/s
$(w_L)_{out}$ = mass-flow rate of outlet liquid, kg/s
$(w_L)_{rb}$ = mass-flow rate of liquid at the riser base, kg/s
$(w_L)_{wh}$ = mass-flow rate of liquid at the wellhead, kg/s
z_1 = normalized valve opening, –
Z = compressibility factor, –
Z_1 = choke valve opening, %
α_L = liquid volume fraction, m^3/m^3
$\alpha^m{}_L$ = liquid mass fraction, kg/kg
$(\alpha_L)_{rb}$ = liquid volume fraction at the riser base, m^3/m^3
$(\alpha_L)_{rt}$ = liquid volume fraction at the top of the riser, m^3/m^3
$(\alpha_L)_{wb}$ = liquid volume fraction at the bottom of the well, m^3/m^3
$(\alpha_L)_{wt}$ = liquid volume fraction at the top of the well, m^3/m^3
$\langle \alpha_L \rangle_p$ = average liquid volume fraction in the pipeline, m^3/m^3
$\langle \alpha_L \rangle_r$ = average liquid volume fraction in the riser, m^3/m^3
$\langle \alpha_L \rangle_w$ = average liquid volume fraction in the well, m^3/m^3
$\langle \alpha^m_G \rangle_{wt}$ = gas mass fraction at the top of the well, kg/kg
$\langle \alpha^m_L \rangle_{rt}$ = liquid mass fraction at the top of the riser, kg/kg
$\langle \alpha^m_L \rangle_p$ = average liquid mass fraction in the pipeline, kg/kg
γ = coefficient used to fine tune the model, –
$(\Delta P_f)_p$ = frictional pressure loss in the pipeline, Pa
$(\Delta P_f)_r$ = frictional pressure loss in the riser, Pa
$(\Delta P_f)_w$ = frictional pressure loss in the well, Pa
ΔP_G = differential pressure for gas flow at the riser base, Pa
ΔP_L = differential pressure for liquid flow at the riser base, Pa
λ_p = riction factor in the pipeline, –
λ_r = friction factor in the riser, –
λ_w = friction factor in the well, –
$\langle \mu_m \rangle_p$ = average mixture viscosity in the pipeline, Pa·s
$\langle \mu_m \rangle_r$ = average mixture viscosity in the riser, Pa·s
$(\rho_G)_p$ = gas density in the pipeline, kg/m^3
$(\rho_G)_r$ = gas density in the riser, kg/m^3
$(\rho_G)_w$ = gas density in the well, kg/m^3
$\langle \rho_G \rangle_p$ = average gas density in the pipeline, kg/m^3
$\langle \rho_m \rangle_p$ = average mixture density in the pipeline, kg/m^3
$\langle \rho_m \rangle_r$ = average mixture density inside the riser, kg/m^3
$\langle \rho_m \rangle_w$ = average mixture density in the well, kg/m^3
ρ_{rt} = mixture density at the top of the riser, kg/m^3
ρ_{wt} = mixture density at the top of the well, kg/m^3
ω_c = critical frequency of slugging oscillations, s^{-1}

References

Ahmed, T. 2006. *Reservoir Engineering Handbook*, third edition. Oxford, UK: Elsevier.

Bendiksen, K.H., Malnes, D., Moe, R. et al. 1991. The Dynamic Two-Fluid Model OLGA: Theory and Application. *SPE Prod Eng* **6** (2): 171–180. SPE-19451-PA. http://dx.doi.org/10.2118/19451-PA.

Brill, J.P. and Beggs, H.D. 1991. *Two-Phase Flow In Pipes*, sixth edition. Tulsa, Oklahoma: University of Tulsa.

Courbot, A. 1996. Prevention of Severe Slugging in the Dunbar 16” Multiphase Pipeline. Presented at the Offshore Technology Conference, Houston, 6–9 May. OTC-8196-MS. http://dx.doi.org/10.4043/8196-MS.

Di Meglio, F., Kaasa, G.-O., and Petit, N. 2009. A first principle model for multiphase slugging flow in vertical risers. In *Proceedings of the 48th IEEE Conference on Decision and Control,* held jointly with the 28th

Chinese Control Conference, 15–18 December, Shanghai, China, 8244–8251. http://dx.doi.org/10.1109/CDC.2009.5400680.

Di Meglio, F., Kaasa, G.-O., Petit, N. et al. 2010. Reproducing slugging oscillations of a real oil well. In *49th IEEE Conference on Decision and Control,* 15–17 December, Atlanta, Georgia, USA, 4473–4479. http://dx.doi.org/10.1109/CDC.2010.5717367.

Drew, T.B., Koo, E.C., and McAdams, W.H. 1932. The Friction Factor for Clean Round Pipes. *Trans AICHE* **28**: 56–72.

Dukler, A.E., Wicks, M., and Cleveland, R.G. 1964. Frictional pressure drop in two-phase flow: A. A comparison of existing correlations for pressure loss and holdup. *AIChE Journal* **10** (1): 38–43. http://dx.doi.org/10.1002/aic.690100117.

Eikrem, G.O. 2008. Eikrem riser model. http://www.nt.ntnu.no/users/skoge/diplom/prosjekt08/tuvnes/.

Fard, M.P., Godhavn, J.M., and Sagatun, S.I. 2006. Modeling of Severe Slug and Slug Control With OLGA. *SPE Prod & Oper* **21** (3): 381–387. SPE-84685-PA. http://dx.doi.org/10.2118/84685-PA.

Godhavn, J.M., Fard, M.P., and Fuchs, P.H. 2005. New slug control strategies, tuning rules and experimental results. *Journal of Process Control* **15** (5): 547–557. http://dx.doi.org/10.1016/j.jprocont. 2004.10.003.

Haaland, S.E. 1983. Simple and Explicit Formulas for the Friction Factor in Turbulent Pipe Flow. *J. Fluids Eng.* **105** (1): 89–90. http://dx.doi.org/10.1115/1.3240948.

Havre, K., Stornes, K.O., and Stray, H. 2000. Taming slug flow in pipelines. *ABB Review* **4**: 55–63.

Hu, B. and Golan, M. 2003. Gas-lift Instability Resulted Production Loss and Its Remedy by Feedback Control: Dynamical Simulation Results. Presented at the SPE International Improved Oil Recovery Conference in Asia Pacific, Kuala Lumpur, 20–21 October. SPE-84917-MS. http://dx.doi.org/10.2118/84917-MS.

Jahanshahi, E. 2012. MATLAB codes for slug models. http://www.nt.ntnu.no/users/skoge/software/slug-models-jahanshahi/.

Jahanshahi, E. and Skogestad, S. 2011. Simplified Dynamical Models for Control of Severe Slugging in Multiphase Risers. In *World Congress*, eds. S. Bittanti, A. Cenedese, and S. Zampieri, Vol. 18, Part 1, 1634–1639. http://dx.doi.org/10.3182/20110828-6-IT-1002.00981.

Jahanshahi, E., Skogestad, S., and Helgesen, A.H. 2012. Controllability Analysis of Severe Slugging in Well-Pipeline/riser Systems. In *Automatic Control in Offshore Oil and Gas Production*, ed. L. Imsland, Vol. 1, Part 1, 101–108. http://dx.doi.org/10.3182/20120531-2-NO-4020.00014.

Kaasa, G.-O., Alstad, V., Zhou, J. et al. 2008. Attenuation of Slugging in Unstable Oil Wells by Nonlinear Control. In *World Congress*, eds. M.J. Chung and P. Misra, Vol. 17, Part 1, 6251–6256. http://dx.doi.org/10.3182/20080706-5-KR-1001.01055.

Khalil, H.K. 2002. *Nonlinear Systems*, third edition. Upper Saddle River, New Jersey: Prentice Hall.

Martins da Silva, C., Dessen, F., and Nydal, O.J. 2010. Dynamic Multiphase Flow Models for Control. Presented at the 7th North American Conference on Multiphase Technology, Banff, Canada, 2–4 June. BHR-2010-F2.

Skogestad, S. 2009. *Chemical And Energy Process Engineering*. Boca Raton, Florida: CRC Press.

Storkaas, E. and Skogestad, S. 2007. Controllability analysis of two-phase pipeline/riser systems at riser slugging conditions. *Control Engineering Practice* **15** (5): 567–581. http://dx.doi.org/10.1016/j.conengprac.2006.10.007.

Storkaas, E., Skogestad, S., and Godhavn, J.M. 2003. A low-dimensional dynamic model of severe slugging for control design and analysis. In *Proc.,* 11th International Conference on Multiphase Flow, San Remo, Italy, 117–133. BHR Group.

Taitel, Y. 1986. Stability of severe slugging. *International Journal of Multiphase Flow* **12** (2): 203–217. http://dx.doi.org/10.1016/0301-9322(86)90026-1.

Tuvnes, H. 2008. Final Year Project: Severe Well Slugging and Reservoir-Well Interactions, Modeling and Simulations. Technical report, Norwegian University of Science and Techology.

Wei, J. 1975. Least Square Fitting of an Elephant. *Chemtech* **5** (2): 128–129.

Esmaeil Jahanshahi is a software development engineer at Siemens. Previously, he was a PhD degree candidate at the Norwegian University of Science and Technology (NTNU), Trondheim, Norway. Jahanshahi's research interests include modeling of two-phase flow in oil production and control-system design and estimation (soft sensing). He has authored or coauthored more than 20 technical papers and holds four patents. Jahanshahi holds an MSc degree in instrumentation and automation engineering from the Petroleum University of Technology (Iran) and a PhD degree in chemical engineering from NTNU.

Sigurd Skogestad is a professor of chemical engineering at the NTNU. His research interests include the use of feedback as a tool to make the system well-behaved (including self-optimizing control); control structure design and plantwide control; and distillation column design, control, and dynamics. Skogestad has coauthored more than 200 journal papers and 200 conference papers. He holds an MSc degree in chemical engineering from NTNU and a PhD degree from California Institute of Technology.